



HAL
open science

Experimental Modeling of Seawater Electromagnetic Flow Control

Jean-Paul Thibault, Lionel Rossi

► **To cite this version:**

Jean-Paul Thibault, Lionel Rossi. Experimental Modeling of Seawater Electromagnetic Flow Control. ERCOFTAC Bulletin, 2000, 44. hal-02546991

HAL Id: hal-02546991

<https://hal.science/hal-02546991>

Submitted on 19 Apr 2020

HAL is a multi-disciplinary open access archive for the deposit and dissemination of scientific research documents, whether they are published or not. The documents may come from teaching and research institutions in France or abroad, or from public or private research centers.

L'archive ouverte pluridisciplinaire **HAL**, est destinée au dépôt et à la diffusion de documents scientifiques de niveau recherche, publiés ou non, émanant des établissements d'enseignement et de recherche français ou étrangers, des laboratoires publics ou privés.

Experimental Modeling of Seawater Electromagnetic Flow Control

Jean-Paul Thibault and Lionel Rossi

LEGI, BP 53, 38041 GRENOBLE, France

jean-paul.thibault@hmg.inpg.fr

lionel.rossi@hmg.inpg.fr

ERCOFTAC Bulletin on "Turbulence Control"
March 2000

1 INTRODUCTION

This contribution deals with the concept of using in combination "wall-flush" electrodes and "sub-surface" magnets to create directly local body forces within a seawater boundary layer. The distribution of body forces is managed either for drag reduction or local prevention of specific events like for instance flow separation.

It seems now well admitted in the literature, that coherent motion in the boundary layer is one of the main phenomena involved in turbulence production. As a matter of fact most of turbulent energy can be found in a boundary layer in specific events like sweeps and bursts. These events are responsible for strong velocity fluctuation and consequently increasing drag. In addition they are quasi cyclic and can not survive without a link between them. This concept explaining wall-turbulence self-sustaining is well described for instance by Robinson [1]. Other authors, Smith [2] and Adrian & Balachandar [3] give a detail description of structures present in a boundary layer. Finally hairpin structures seem to be the potential link (in time and space) between turbulent events. A method to produce periodically hairpin structure in an originally laminar boundary layer was presented by Acalar & Smith [4]. It allows analyzing the mechanisms of self-regeneration of these hairpin structures.

Electromagnetic flow control permits to act directly within a boundary layer by applying directly local Lorentz (body) forces. These $\mathbf{j} \times \mathbf{B}$, forces are produced in combination by "wall-flush" electrodes (\mathbf{j} , DC current supply) and "sub-surface" permanent magnets (\mathbf{B} , magnetic induction origin). The resulting forces can act directly on velocity and vorticity components in the flow, close to the wall. Mainly two configurations are described in the literature depending on the geometry of electrodes and magnets. First the wall-normal geometry where electrodes and magnets form a square pair by pair (see figure 1). In this case the

forces are mostly wall-normal. Second the parallel geometry where electrodes and magnet are parallel like in Henoach & Stace [5] and Weier et al. [6] papers (see Figure 2). In this case the forces are mostly wall-parallel.

In this paper wall-normal shape is considered and a group of two permanent magnet poles and two electrodes is called EM actuator. Firstly, a rapid description of EM actuators is made before a presentation of basic equations, and the simplifications used to identify driving terms and modes of action on boundary layer. Secondly experimental results will show some mechanism of EM control.

In order to present a step-by-step comprehensive model of the possible mechanisms involved in ElectroMagnetic flow control the present paper is based on the conception of elementary models. These models may be multiplied and upgraded to give an actual description of a very complex reality. They are first used in a comprehensive way and second they are integrated to a more predictive scheme.

2 BRIEF DESCRIPTION OF EM ACTUATORS

Figure 1 represents a wall normal EM actuator. The top view represents both magnets (N and S) and electrodes (+ and -). In the lower view, electromagnetic forces are schematized. They are mainly directed normal to the wall in addition the vorticity ($\mathbf{curl} \mathbf{j} \times \mathbf{B}$) associated is also represented above the magnets.

Experimental demonstration of the effect of single wall-normal EM actuator as well as an array of them was first presented by Nosenchuck & Brown [7]. A significant turbulent intensity reduction and drag reduction was measured. Unfortunately, it seems that due to its complexity the mechanism of action was poorly understood.

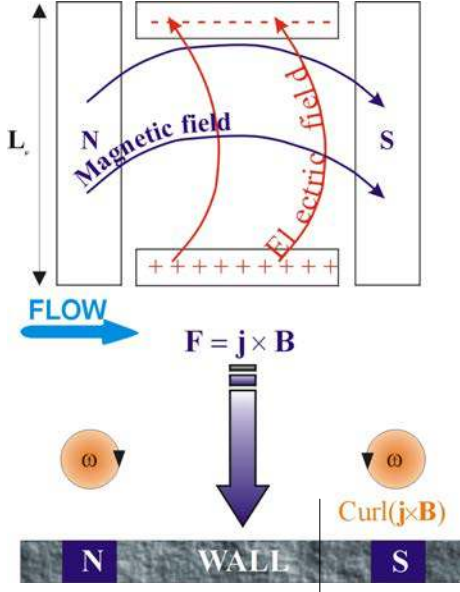


Figure 1 : Wall normal EM actuator, Electric field, Magnetic field, Lorentz forces and imposed EM vorticity

Figure 2 represents an EM actuator, where electrodes and magnet are both parallel to the mean flow direction. Consequently EM forces are also parallel to the wall. The electromagnetic body force can be used to locally balance an axial pressure gradient that could else create a flow separation. In the mean time axial forces are able to create wall-jets associated with turbulent intensity reduction. Henoach & Stace [5] and Weier et al [6] gave experimental demonstration of flow separation prevention as well as turbulent intensity reduction using this parallel configuration of EM flow control.

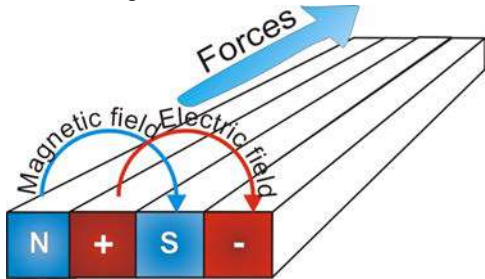


Figure 2 : Wall parallel EM actuator.

In both cases, action at a scale of order of the boundary layer is necessarily based on the use of a network of EM actuator each of them having a scale based on magnets and electrode spacing. In the parallel configuration this network can be supplied by DC currents, while in the wall-normal configuration multiple DC pulsed currents are more appropriate. When a global control process is used the network, (similar to a chessboard) is supplied by a multiphase (i.e. four) pulse of current having a base-frequency varying proportionally to the mean flow velocity Nosenchuck [9]. In the case of local (closed-loop) control, measurements of flow fluctuation (i.e. local pressure) and feedback actuation are required. Each actuator of the network is supplied by a current pulse simultaneously to a turbulent related event (for example pressure burst) is

detected. Kim, [10] [11], Meng [12] [13], proposed some models and approaches for active control of turbulent boundary layer in the aim to obtain drag reduction. Approaches presented by Kim in [11] are both in closed loop feed back control and open loop control.

3 SOME POSSIBILITIES OF FLOW CONTROL BY EM ACTUATOR

3.1 Basic equations

Flow equations appropriate to EM flow control include additional Lorentz forces and additional vorticity terms: EM vorticity, see

Figure 1. Thus Navier Stokes equation and vorticity equation are both changed as following:

Navier Stokes equation:

$$\rho \frac{d\mathbf{U}}{dt} + \nabla P + \rho \mathbf{g} = \mu \nabla^2 \mathbf{U} + \mathbf{j} \times \mathbf{B} \quad \text{Equation 1}$$

Vorticity equation:

$$\rho \frac{d\boldsymbol{\omega}}{dt} = \rho \boldsymbol{\omega} \cdot \nabla \mathbf{U} + \mu \nabla^2 \boldsymbol{\omega} + \nabla \times (\mathbf{j} \times \mathbf{B}) \quad \text{Equation 2}$$

$\mathbf{j} \times \mathbf{B}$ and $\nabla \times (\mathbf{j} \times \mathbf{B})$ are terms controlled by EM actuator. They clearly exhibit that electromagnetic control has two complementary ways to act directly on the hydrodynamics of the boundary layer by changing velocity and vorticity fields.

Regarding the magnetic induction equation, because permanent magnets are used and the flow is very poorly conducting, \mathbf{B} is permanent and independent of the flow ($R_m \sim 10^{-6}$). Then it is clear that no power is needed for sustaining the magnetic field.

Finally magnetic induction equation reduces simply to a Laplace equation because time dependant terms as well as magnetic convection are negligible.

Induction equation :

$$\nabla^2 \mathbf{B} = 0 \quad \text{Equation 3}$$

Regarding current density, \mathbf{j} , the Ohm's law is the constitutive equation. It demonstrate the "competition" between applied electric field \mathbf{E} (due to electrode voltage drop) and the induced electric field $\mathbf{u} \times \mathbf{B}$ (due to the motion of the conducting flow in the magnetic field).

Ohm's law :

$$\mathbf{j} = \sigma (\mathbf{E} + \mathbf{u} \times \mathbf{B}) \quad \text{Equation 4}$$

In the case of seawater flow control, because a very poor apparent electrical conductivity of the flow, $\mathbf{u} \times \mathbf{B}$ is small in front of \mathbf{E} , with a ratio of 10^{-2} in most of the flow domain. Here we choose to maintain $\mathbf{u} \times \mathbf{B}$ terms in the Ohm's law, because it can plays a role in a region very close to the wall. Finally the value of \mathbf{j} is mostly equal to $\sigma \mathbf{E}$.

It is important to notice that in the present work, EM flow control in seawater, the applied electric field directly imposes and control the Lorentz forces. Current density, \mathbf{j} , is used as the adjustable parameter of the process, it controls the intensity of $\mathbf{j} \times \mathbf{B}$ forces and vorticity. Its energetic coast is proportional to \mathbf{j}^2 while \mathbf{B} is power free as already mentioned. Consequently \mathbf{B} magnitude has to be as high as possible (considering the limits of permanent magnet technology) and \mathbf{j} has to be large enough to produce the needed forces to control the flow.

3.2 Dimensionless analysis of a single EM actuator

A selection of dimensionless numbers can be examined in order to identify the possible dominant mechanism of EM control in seawater. This analysis may provide a first step in the understanding of EM actuators regarding their typical dimensions. Note that the following typical scales chosen apply to the presented experiments : length of actuator $L_{EM} \sim 10^{-2}$ m, magnetic induction $B \sim 1$ T, imposed electric field $E \sim 10^3$ Vm^{-1} , electric conductivity of seawater $\sigma \sim 5$ S/m, magnetic permeability $\mu = 4\pi \cdot 10^{-7}$ Hm^{-1} , flow velocity $U \sim 1$ to 10 ms^{-1} , boundary layer thickness $\delta \sim 10^{-3}$ to 10^{-2} m, consequently we obtain typical Reynolds magnetic number: $R_m \sim 10^6$ and Reynolds numbers: $R_{ex} > 10^6$.

Hartmann number:

H_a , Hartmann number is the ratio of EM driving terms to viscous terms. The two typical length-scales selected are respectively : the boundary layer thickness, δ , and the length of action of EM forces, $L/5$. Both limit cases are considered.

$$\partial \frac{L}{5} \gg \delta \quad \text{Then } H_a^2 = \frac{\sigma E B \delta^2}{\rho \nu U}$$

With $\delta \sim 10^{-3}$ m and $L_{EM} \sim 10^{-2}$ m we found that H_a is in order of 1.

$$\bullet \delta \geq \frac{L}{5} \quad \text{Then } H_a^2 = 0.675 \frac{\sigma E B (L/5)^2}{\rho \nu U \left(\frac{L/5}{\delta} \right)^{1/7}}$$

Last equation takes into account the mean value of E and B , in the layer thickness of main EM forces magnitude, and a puissance 1/7 evolution of mean velocity in the boundary layer. With $\delta \sim 10^{-2}$ m and $L_{EM} \sim 10^{-3}$ m we found that H_a is in order of 1.

In both case we found that: $H_a \approx 1$. This dimensionless evaluation shows that EM terms can have the same order than viscous terms when considering it at the local scale of an EM actuator.

Interaction parameter:

I , interaction parameter, is the ratio of EM forces to inertia forces. Here a novel attempt (in MHD) is made by defining three interaction parameters. Each case is constructed on different scales of velocity and length.

← The first, I_U , is constructed on the mean flow velocity and the turbulent boundary layer thickness.

$$I_U = \frac{\sigma E B}{\rho \frac{U^2}{\delta}} = \frac{\sigma E B \delta}{\rho U^2} \approx 10^{-4} \text{ to } 10^{-2}$$

It shows that EM forces are not able to compete with inertia of the bulk flow.

↑ The second, I_V , is constructed on perspiration velocity, V , and on typical size of EM actuator.

$$I_V = \frac{\sigma E B}{\rho \frac{V^2}{L}} = \frac{\sigma E B L}{\rho V^2} \approx 10^3 \text{ to } 10^5$$

It shows that wall normal Lorentz forces are capable of dominating normal velocity. So injection of Lorentz forces in the boundary layer can completely change the profile of normal velocity.

→ The third, I_{vloc} , is constructed on a turbulent velocity and a scale of local event.

$$I_{vloc} = \frac{\sigma E B}{\rho \frac{v^2}{l}} = \frac{\sigma E B l}{\rho v^2} \approx 10^{-4} \text{ to } 10^{-1}$$

I_{vloc} is the interaction parameter based on a fluctuation velocity, 10% of U , and typical length of a local turbulent events, l (100^+). This interaction parameter show that the control of an individual hairpin structure by a single EM actuation would need a much higher current density than the one considered here.

This analysis of typical dimensionless numbers clearly demonstrates that EM control is more proper to act on the flow at the typical length-scale of the boundary layer (i.e. around a turbulent event) than to act directly on a turbulent event. This remark points out the two strategies of control considered in the literature. First global EM control which acts with (multiple shots) around a turbulent event by reorganizing locally the turbulent boundary layer while the flow develops along the wall. Second local EM control that detects and acts (single shot) on a turbulent event to “kill” it quasi immediately. These two types of control process are coherent with different size of actuator and different physics to be efficient. It means for instance that the actuation can be periodic in global EM, but has to be actively controlled in local EM.

3.3 Effect of network for multiple EM actuators

Beyond the analysis of dimensionless numbers of a single EM actuator, it is interesting to analyze an EM actuator network. Each EM actuator contributes to change the flow owing to a cumulative effect of suction, see Figure 3. Consequently the wall normal velocity within the boundary layer is changed and, due to flow conservation, wall jets appear. Theses wall jets (normal in the outer region and parallel to the wall in the inner part), take place in a low speed region of the boundary layer. Consequently it can play locally a dominant role on the near wall flow.

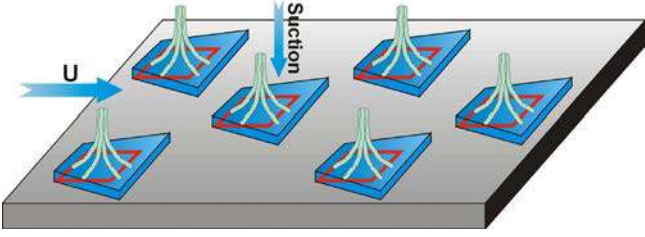


Figure 3 : Network of EM actuators, suction and wall jet.

Electromagnetic control is thus able to change the flow on and between coherent structures (i.e. hairpins). The network of EM actuator creates a new environment for structures. This mechanism is proposed here to explain the delay or suppression of transition to turbulence of the boundary layer. When this EM control is applied downflow the production of coherent structures, it places these structures in a context where they cannot survive. Structures may vanish or decrease because they are simply crushed to the wall or because their regeneration process is broken.

4 BASIC MECHANISMS AND EXPERIMENTAL MODELING OF AN EM ACTUATOR

Various strategies can be selected to make an experimental approach having the aim of understanding EM flow control. Here a step-by-step analytical procedure is chosen.

First part of this paper has dealt with generality and an evaluation of the possible action of EM actuator on a boundary layer. This part introduces more precisely basic mechanisms of an EM actuator. First an identification of driving terms of EM actuator (local components of electric field and induction, local components of forces and vorticity) will be analytically discussed. Second an experimental approach allows analyzing EM actuator action based on visualization of injected vorticity, identification of action zones depending on power supply. Consequently three control mechanisms shown by experiences are presented. Third an experiment in a small seawater tunnel demonstrates the action of EM control on coherent hairpin structures generated by a wall flush half sphere.

4.1 Analytical identification of driving terms

The electromagnetic fields developed above an EM actuator are completely 3-dimensional. In order to get a qualitative understanding of electric field and magnetic field distributions let us consider various zones of the domain above an EM actuator, see Figure 4. The following global descriptive remarks on electromagnetic fields is useful for a better understanding of their distribution: 1) Magnetic field and electric field are both decreasing from the wall to the external flow. 2) Magnetic field is mostly wall normal on magnet poles and longitudinal above the center of the actuator. 3) Electric field is mostly wall normal at electrode surface and transversal above the center of the actuator.

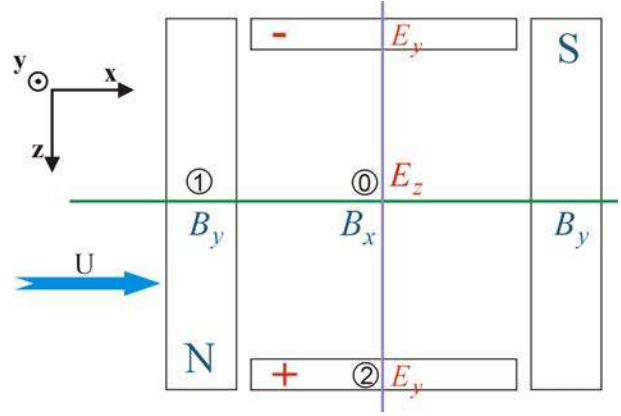


Figure 4 : Various zones above the EM actuator and dominant components of electromagnetic fields.

The three zones (0, 1, 2) marked on figure 4 correspond to specific regions above the EM actuator where either magnetic or electric field have a dominant component. Zone 0 corresponds to the center of the actuator. Zone 1 corresponds to the (x,y) plan that is median of 2 electrodes. Zone 2 corresponds to (y,z) plan that is median to 2 magnets.

As mentioned previously the current density is proportional to electric field (deriving from electric potential) by a factor σ (apparent electrical conductivity of the flow). A complementary hypothesis is used here. Based on the long extend of magnet poles the magnetic field is considered as 2D. Consequently the B_z component of magnetic field is zero, due to EM actuator orientation with respect to the main flow direction x, see figure 1. Finally a very good estimate of Lorentz forces is the following:

$$\mathbf{j} \times \mathbf{B} \cong \sigma \mathbf{E} \times \mathbf{B} = \sigma \begin{vmatrix} -B_y E_z \\ B_x E_z \\ B_y E_x - B_x E_y \end{vmatrix}$$

Equation 5

Considering Equation 5, in the three zones described in figure 4, a qualitative description of Lorentz forces above the actuator is possible see figure 5.

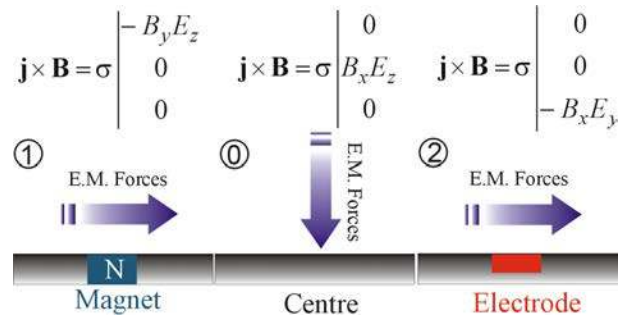


Figure 5 : Lorentz forces distribution in the three zones described in figure 4.

To summarize EM forces above the actuator have a quasi-concentric distribution. The module of forces is increasing toward the wall and is maximal at the wall, above center and electrodes.

Considering now the imposed EM vorticity: $\text{curl}(\mathbf{j} \times \mathbf{B})$ a good approximation is following :

$$\nabla \times (\mathbf{j} \times \mathbf{B}) \cong \sigma \begin{vmatrix} \frac{\partial}{\partial y} (B_y E_x - B_x E_y) - B_x \frac{\partial E_z}{\partial z} \\ -\frac{\partial}{\partial x} (B_y E_x - B_x E_y) - B_y \frac{\partial E_z}{\partial z} \\ B_x \frac{\partial E_z}{\partial x} + B_y \frac{\partial E_z}{\partial y} \end{vmatrix}$$

Equation 6

Equation 6 is obtained with equation 5 combined to equations of conservation of current and magnetic field.

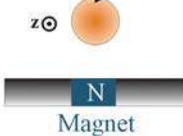

$\textcircled{1} \quad \nabla \times (\mathbf{j} \times \mathbf{B}) = \sigma \begin{vmatrix} 0 \\ 0 \\ B_x \frac{\partial E_z}{\partial x} + B_y \frac{\partial E_z}{\partial y} \end{vmatrix}$ <p>Transversal vorticity Aloof maximum</p> 	$\textcircled{2} \quad \nabla \times (\mathbf{j} \times \mathbf{B}) = \sigma \begin{vmatrix} -E_y \frac{\partial B_x}{\partial y} \\ 0 \\ 0 \end{vmatrix}$ <p>Longitudinal vorticity Wall maximum</p> 
--	---

Figure 6 : Imposed EM vorticity in various zone described in figure 4.

The following comments are derived considering equation 6 in the zones previously described. The imposed vorticity is zero in the center, it is transversal with a maximum aloof from the wall above magnets and it is longitudinal with a maximum at the wall above electrodes (in the actuator orientation chose in

Figure 1). This description could be consid as coherent with the concept of “vorticity ring” of vorticity presented by Nosenchuck 1997 [14]. This ring is aloof from the wall above magnet and near the wall above electrodes which is coherent with figure 6. But the experiments described latter show that the real situation is more complicated than a simple vorticity ring.

4.2 Experimental characterization of the flow above an EM actuator in an aquarium

Experiments presented are realized with a wall normal EM actuator whose typical size is 3 cm (square border). Electrodes are “wall-flush” and made of titanium coated with platinum, the surface of one electrode is 76 mm². “Sub surface” permanent magnets (made of rare hearth material) produce a induction of 1.3 T at the pole surface. Figure 7 is a photo of EM actuator used for our experimental investigations.

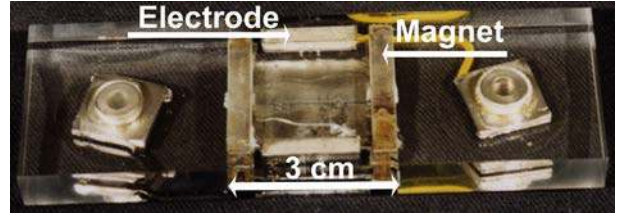


Figure 7 : EM actuator

In the first series of experience, EM actuator is placed flush in a 40 cm in vertical plate, which is entirely immersed in an aquarium (flow at rest) filled with saltwater (35g/l NaCl). The flow visualizations are obtained by “dye injection” using multiple fluoresceine injection and particle tracing.

4.2.1 Vorticity and wall jets

Figure 8 is a cut view (plan x,y) of the two vortical structures produced above the magnets (actuator at top) . Figure 9 is a cut view of one of the vortical structure marked by particles (actuator at bottom).

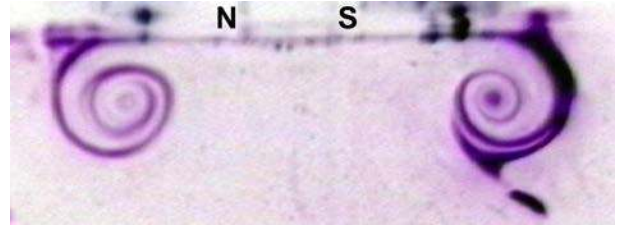


Figure 8 : Cut view (plan x,y) of the vortical structures produced by the EM actuator (actuator at the top marked by N & S magnets).

These cut views confirm the previous analytical calculation and shows that imposed vorticity may really be one of the mechanisms involved in electromagnetic control process.

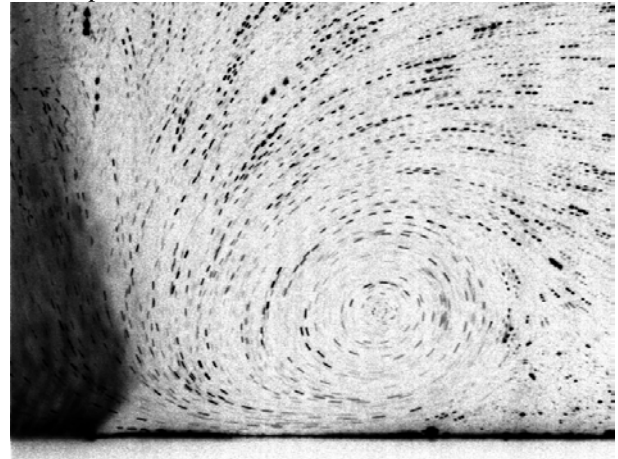


Figure 9 : Cut view of vortical structure and wall-jet (particle tracing, actuator at bottom)

The visualisation process is also useful to show the entire distribution of imposed vorticity. The technique is to prepare the visualisation by filling a pyramidal flow volume above the EM actuator. Fluoresceine marks this flow volume and is filled in by seven holes in the wall. When the flow volume is marked, we stop fluoresceine injection and switch on the EM actuator. The EM forces

pump the marked flow and redistribute it above EM actuator. All visualisations presented are obtained with EM forces mostly positive toward the wall (suction).

Figure 10 is a time series of front view of the actuator inserted in a vertical “black-wall”. The typical size of each view is 30 cm *60 cm. Typical size of the entire vortical structure is starting at the scale of the actuator 3cm*3cm and it extends up to 20cm*30cm after 6s. Electrodes are horizontal and can be seen in the centre. Undesired electrolysis bubbles alter the marking of upper part of vortical structure. Nevertheless rotations of the actuator have demonstrated that the 4 vorticity tubes are generated independently of the bubbles.

Results of this experimental realisation are quite surprising. The perfect ring of vorticity previously mentioned is not observed. In fact four tubes of vorticity develop along time (see figure 10). Two straight transversal tubes (parallel to the magnets poles) with vorticity generated above magnet, and two tubes of vorticity with horse-shoe shape (“parallel” to the electrode) generated in the region above electrodes. These tubes of vorticity are connected in “mushroom like” shape.

Evolution of vortical structure seems to be due to two phenomena. First a transport of two vortexes near to the wall. Second convection by the flow (wall-normal jet), due to suction and redistribution of wall-normal velocity in wall-parallel jets, due to flow conservation. The region of interaction of vortex tubes (at corners) is also interesting because in that region diagonal wall jets are observed. These jets have very strong dynamics in the same diagonal where the mushroom shape is observed.

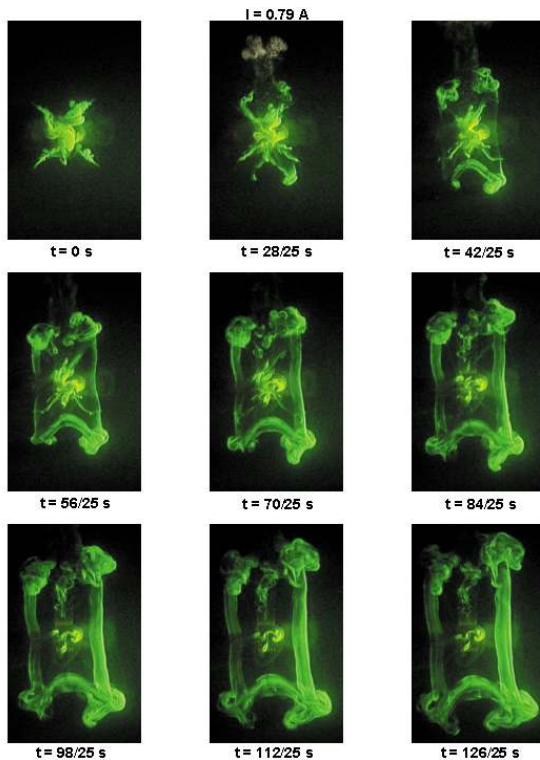


Figure 10 : Time evolution of the vortical structure developing above the EM actuator (front view).

Figure 11 is a cut view of particle tracing in the diagonal region previously observed on the front views. This picture shows diagonal jets (white bottom part of the figure), it demonstrates its very high dynamics.

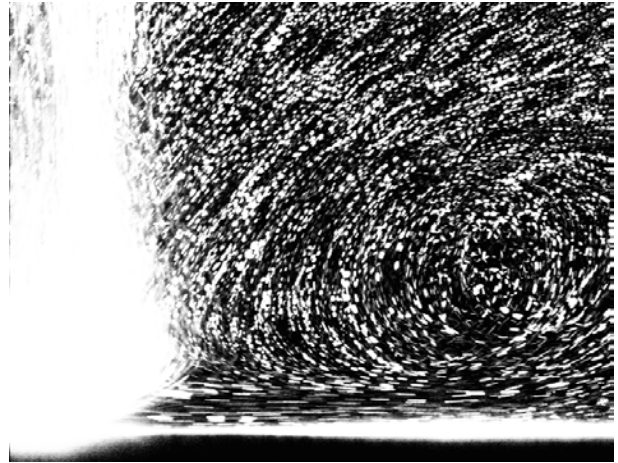


Figure 11 : Cut view of a diagonal wall-jet (particle tracing, actuator at bottom)

The conceptual explanation for these diagonal jets is that there is a lack of EM forces in the angles due to the decrease of both electric and magnetic fields. The center of actuator is a region of high pressure due to wall-normal jet breaking. This high pressure is balanced by the Lorentz forces above electrodes as well as above magnets. In the corners due to the vanishing of Lorentz forces, the high pressure is no more balanced and it drives wall jets. An other particularity showed by experiences in aquarium is a spiraled suction in the central zone, see Figure 12.

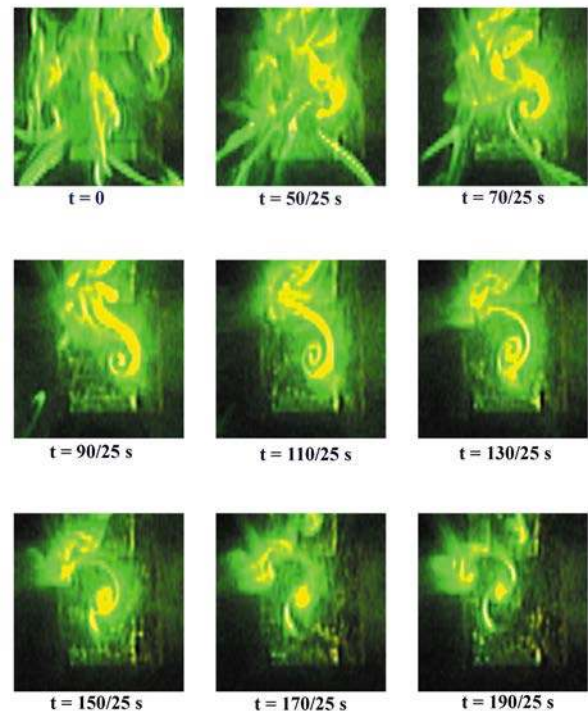


Figure 12 : Spiraled suction in central zone above the EM actuator (front view).

There is no central vortex but some kind of columns of suction where fluoresceine or hydrogen bubbles are captured. These columns move between the different quarters of the central zone.

4.2.2 Suction and action zone

Lorentz forces are mainly positive toward the wall (suction of fluid). There is a zone where Lorentz forces are present with strong intensity and additionally due to flow continuity a zone where Lorentz forces are not directly acting but they are responsible for the observed flow induced, see Figure 13.

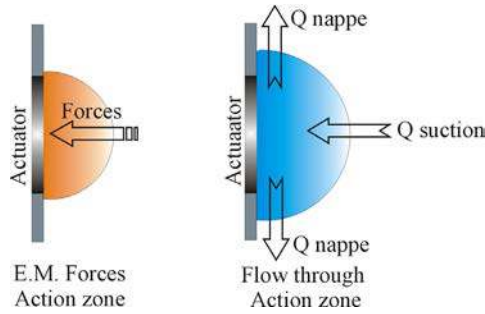


Figure 13 : Description of the action zones respectively to forces and flow induced.

The zone where forces are dominant is smaller than the zone where the fluid is pumped. Thus the distance of effects seems to be quite more important compare to the typical length of decay of induction and electric fields. Basically EM forces are confined in a zone having the typical size of the actuator but suction effect appear to pump the flow in a larger domain. In a static tank, for 0.8s power supply and 1.2 A of current intensity, the distance of action is of order of 3 times the actuator typical size.

To study actuator effect on suction, we have performed a series of tests using local injection of fluoresceine through a vertical mini-tube producing a laminar fluoresceine jet having velocity of order of 3 mm/s and a 1.2 mm diameter. This tracing tube is placed parallel to the wall, its orifice on the central normal of the actuator, at a distance y from the wall. The latter is the only variable distance of the experiment. Then it is possible to analyze for various activation time pulses (0.1s, 0.2s, 0.3s, 0.4s, 0.6s, 0.8s, 10s) the evolution of the distance at which the tracing jet is sucked (or not) by the flow induced by the EM actuator. This distance is so called : distance of action.

Distance of action is increasing with the electric power as well as the time of actuation, see Figure 14, so there is at least two mechanisms to consider: First, increasing of forces makes a stronger suction that's to say an increased distance of action. Second, effect of forces injection is increasing with time of power supplying and consequently flow response is increasing with action time of EM forces.

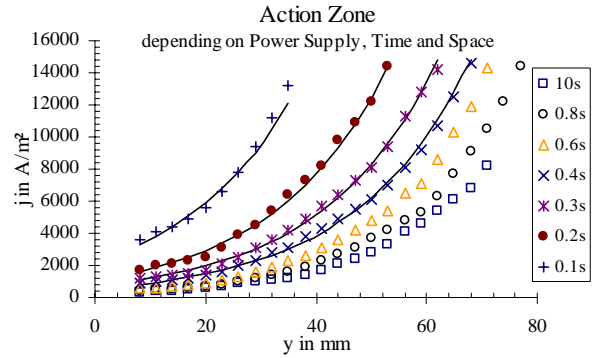


Figure 14 : Distance of effect of EM actuator on punctual injection of 3mm/s speed

Noticing that the energetic coast depends on j^2 , it is clear that, for a given distance of action, the optimized time of action or the optimized power is changing with j . Consequently regarding the control of a real flow, actuation times and power supply have to be optimized jointly. In the case of global control (open loop) due to the flow motion above the actuator, the pulses must be shorter than the typical time of residence of a flowing structure above the actuator. But in addition considering energetic optimization this actuation time has to be optimized coherently with intensity of the applied current.

It is clear that typical flow times (i.e. turn over time and response time to EM forces impulsion) is being really important if the control process is looking for an energetic coast optimization. It is certainly interesting to take advantage of the integration process enable by the use of a network. In this case regarding a structure moving with the “mean” flow in the boundary layer, the effective time of actuation or useful pulse is essentially the summation of the series of pulses injected to a particle during each of its stay above the street of actuators that it passes over. This integration effect may have been observed and called resonance by Nosenchuck 1996 [9]. Experimental demonstration was observed by Boissonneau 1999 [15] who measured an increasing drag reduction along the multiple actuators of a network.

4.3 Experimental characterization of the flow above an EM actuator in a seawater tunnel

In this section, the paper deals with our preliminary test to visualize effects of EM actuator on a boundary layer marked with hairpin like coherent structures. The same EM actuator as previously is now placed is “wall-flush” in the seawater tunnel loop of LEGI, see Figure 15. The test section of our seawater loop is 4cm*4cm with a total length of 1 m and a velocity adjustable up to 10 m/s. The concept here is to analyze the effect of EM actuator on hairpin structures periodically produced downflow a wall hemisphere like in Acalar & Smith [4]. Various hemisphere radius are tested : 4mm, 6mm and 8mm, Thibault et al. [16], Thibault & Rossi [17]. The EM actuator is placed 12 cm down flow the hemisphere. Most of the experiments described are performed for a flow velocity of 8 cm/s.

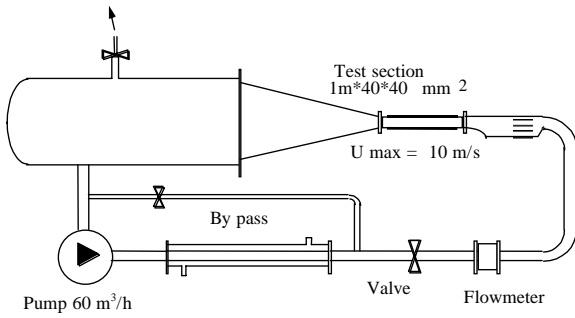


Figure 15 : LEGI Flow control seawater loop.

Figure 16 shows a graphic illustration of principle of present experiment which aims at demonstrating the effect of an EM actuator on structures generated by a wall hemisphere. Some typical values of the experiment are directly indicated on figure 16.

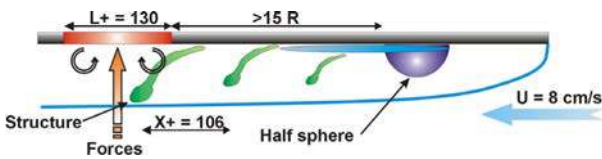


Figure 16 : Principle Hairpin vortices production and actuator interaction

Figure 17 is a visualization tunnel photo (flow comes from right) a street of hairpin structures is generated downflow the hemisphere. The EM actuator inserted in the transparent wall of the tunnel is presently unplugged.

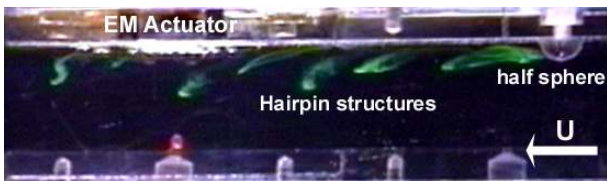


Figure 17 : Visualisation of hairpin street produced by a wall hemisphere (EM actuator unplugged).

Figure 18 shows various effects of the EM control. The structures are turning up or down, depending of the forces sign. In fact previous experiments demonstrate that a laminar boundary layer (without hairpin) is crushed to the wall in a length of order of the size of actuator. In the case of a coherent structures street (like in figure 18) a wall normal motion is initiated above actuator and structure hurts the wall downflow EM actuator. The presence of normal velocity, due to pumping induced by hairpin, may delay the wall normal effect of EM actuator. Due to the fact that body force is acting on and around hairpin it finally drives it to the wall and consequently the structure finally disappears.

The competition between wall normal flow induced by Lorentz forces and by hairpin structure is controlling the time and capability of killing structure by a single shot or multiple (network) shot.

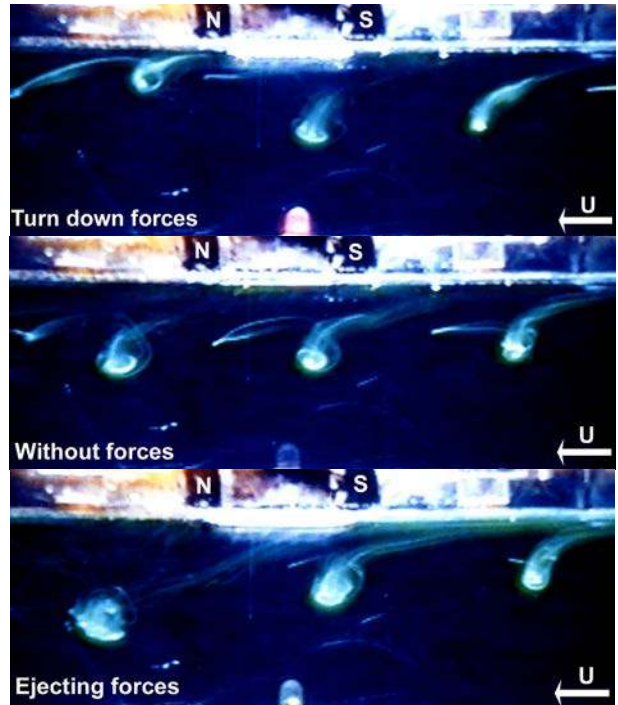


Figure 18 : Action on hairpin structures

It has been observed that with a turn down effect, structures tend to disappear much faster than without EM action. They degenerate very quickly downflow the actuator.

The results presented are only able to validate the concept of this experimental interaction between hairpin structures and EM actuator. Unfortunately due to its very reduced cross section the seawater tunnel is strongly limiting for confinement reasons. A detailed and quantitative analysis is being processed on a larger test-section which is going to be constructed in the near future.

To conclude this part of our experiment, it can be say that preliminary experiments, in seawater tunnel, have shown a real effect of EM actuator. EM actuator is able to alter wall normal velocity and to impose a new motion to the flow. Flow can be turn down or ejected depending on the current polarity. Degeneration of hairpin structures observed downflow a single EM actuator is very encouraging. It clearly motivates our next experiments based on an enlarged seawater tunnel including multiple EM actuators in order to demonstrate the process of time integration of a network and to validate the analysis for optimizing energetic coast.

6 CONCLUSION

EM actuator is a mean to directly apply Lorentz forces in the flow. These local body forces are associated with additional terms in Navier Stokes equation as well as in vorticity equation. Each component of velocity or vorticity is altered by electromagnetic control either directly during actuation or after due to a persisting induced velocity or vorticity.

The analysis of the driving terms of a wall-normal EM actuator indicates that its action is directly and

principally on wall normal velocity. In regions of the boundary layer where normal velocity is weak, EM actuators impose a new component of normal velocity, and in zone where turbulent events introduce wall normal velocity, EM control can counteract by acting on and around these events.

These theoretical interpretations emerge on different possibilities of electromagnetic control. First possibility is to alter turbulence by “killing events” as soon as detected, with a local injection of Lorentz forces. Then coherent motion is directly vanishing, this stops regeneration process and finally induces drag reduction. Second possibility is to process at a large scale using a network producing a street of EM forces moving with a mean velocity fitted to the flow velocity. This way may alter the entire boundary layer to cut down generation and regeneration process and consequently to obtain drag reduction.

Experiments in an aquarium show the presence of vorticity tubes, suction zone with normal velocity, and wall jets with a maximum of velocity in the angles. These three signatures of EM control are linked together because vorticity tube may help suction, then suction induces wall jet, due to wall impermeability. So EM control offers at least three driving mechanism to control the flow.

Experiments using a single EM actuator placed in a small seawater tunnel are presented. This paper reports the action upon a hairpin street produced by a wall flush half-sphere placed up-flow the EM actuator. It is shown that hairpin structures are turn up or down from the wall depending on Lorentz forces sign. In addition a much faster disablement of structures is observed down-flow the EM actuator. The EM actuator is able to impose wall normal velocity component and to control and brake down the development of hairpin structures. In fact, due to its effect in a larger volume than the coherent motion extend, EM actuator acts on and around hairpin. So it is able to drive a hairpin structure nearest to the wall where EM forces are dominant. The local wall normal velocity of hairpin is then controlled by Lorentz forces which are then able to “kill” hairpin structure.

ACKNOWLEDGEMENTS

This work is done in the frame of contracts with the « Délégation Générale de l'Armement » of the French Ministry of Defence.

Special thanks to Mr F.Bonnell (ENSHMG), Dr O. Cugat (ENSIEG-LEG), Dr S. Tardu (LEGI), Mr. P. Carecchio (LEGI) and M. Kusulja (LEGI).

REFERENCES

[1] **ROBINSON ; 1991**, “Coherent motions in the turbulent boundary layer”, *An. Rev. Fluid. Mech.* 23 : 601-39.

[2] **SMITH C.R., 1998**, “Vortex development and interactions in turbulent boundary layers : amplifications for surface drag reduction”, *Proc. of the Int. Symp. on Seawater Drag Reduction, Newport R. I.* 1998, pp 39-45.

[3] **ADRIAN R.J. & BALACHANDAR S., 1998**, “vortex packet and the structure of wall turbulence”, *Proc. of the Int. Symp. on Seawater Drag Reduction, Newport R. I.* 1998, pp 33-38.

[4] **ACALAR, SMITH ; 1987**, « A study of hairpin vortices in a laminar boundary layer part1 : hairpin vortices generated by a hemisphere protuberance », *JFM* (1987) vol 175 pp1-41.

[5] **HENOCH C. & STACE J., 1995**, “Experimental Investigation of a Salt Water Turbulent Boundary Layer Modified by an Applied Streamwise Magnetohydrodynamic Body Force”, *Phys. Fluids* 7,(6) , pp. 1371-1383, June 1995.

[6] **WEIER T., GERBETH G., MUTSCHKE G., PLATACIS E., LIELAUSIS O., 1998**, “Experiments on cylinder wake stabilization in an electrolyte solution by means of electromagnetic forces localized on cylinder surface”, *ELSEVIER, Experimental Thermal and Fluid Science* 16 (1998) pp 84-91.

[7] **NOSENCHUCK D.M. & BROWN G.L. : 1993**, Princeton, “The direct control of wall shear stress in a turbulent boundary layer”, *Proc. of the Int. Conf. on Near Wall Turbulent Flows, Elsevier* pp 689-698.

[8] **BANDYOPADHAY R., 1998**, « Drag reduction experiments on a small axisymmetric body in saltwater using electromagnetic microtiles », *Proc. of the Int. Symp. on Seawater Drag Reduction, Newport R. I.*, pp 457-461.

[9] **NOSENCHUCK D.M., 1996**, “Boundary Layer Control Using the Lorentz Force”, *ASME Fluids Engineering Meeting, San Diego, July 1996*.

[10] **KIM J., 1997**, “Boundary layer control for drag reduction”, invited talk, *Int. workshop, EBLC Dresden 1997*.

[11] **KIM J. 1998**, “Active control of turbulent boundary layers for drag reduction” *IUTAM Symp. on Mechanism of Pasive and Active Flow Control, 1998, September 7-11, Göttingen Germany*.

[12] **MENG J.C.S. ; 1996**, “Wall layer microturbulence phenomenological model and a semi Markov probability predictive model for active control of turbulent boundary layers”, *NUWC Division Newport Technical Digest 1996*.

[13] **MENG J., 1998**, “Engineering insight of near-wall microturbulence for drag reduction and derivation of a design map for seawater electromagnetic turbulence control” », *Proc. of the Int. Symp. on Seawater Drag Reduction, Newport R. I.*, pp389-393.

[14] **NOSENCHUCK D., 1997**, “Electromagnetic Turbulence Control”, *EBLC Workshop, Dresden, Germany, July 1997*

[15] **BOISSONNEAU P., 1999**, MAE dept. Princeton University, Personal communication 1999

[16] **THIBAUT J.P., BOTTON V., ROSSI L. ; 1998**, « Electromagnetic effect on low speed coherent structures embedded in a wall layer », *Proc. of the Int. Symp. on Seawater Drag Reduction, Newport R. I.*, pp389-393.

[17] **THIBAUT J.P., ROSSI L., 1997**, “Seawater MHD: Electromagnetic Flow Control”, *Third Int. Conf. on Transfer Phenomena in Magneto Hydro Dynamic and Electroconducting Flows, vol. 1, pp. 243-248, Aussois, France, 1997*